Determination of true stress strain characteristics of structural steels using Instantaneous Area Method

Determination of true stress strain characteristics of structural steels using Instantaneous Area Method

H C Ho[1,2,3], T Y Xiao[2], C Chen[2], And K F Chung[1,2]

[1]Department of Civil and Environmental Engineering, The Hong Kong Polytechnic University, Hong Kong SAR, PR China
[2]Chinese National Engineering Research Centre for Steel Construction (Hong Kong Branch), The Hong Kong Polytechnic University, Hong Kong SAR, PR China

Email: hc.ho@polyu.edu.hk

Abstract. This paper presents recent research findings on true stress strain characteristics of normal strength S275, S355 and high strength S690 steels to EN 10025:2005. It aims to provide generalized constitutive models for analysis and design of steel structures. Comprehensive experimental and numerical investigations into mechanical properties of the structural steels have been carried out based on test results of nine monotonic tensile tests**.** Non-uniform stress and strain distributions within the necked region are found when the test coupons are under very large deformation. After corrections to the stress and strain non-uniformities by **Instantaneous Area Method** with successive approximations, true stress strain characteristics of the tested steels were successfully quantified as generalized constitutive models. Moreover, the microstructures of the typical structural steels haven been carefully examined, and their microstructural constituents are successfully quantified by Digital Image Analytics. The research findings are very important for subsequent numerical investigations into the structural performance of steel structures under very large deformations up to fracture. The authors are grateful for the financial supports from the Research Grants Council of the Government of Hong Kong SAR, and the CNERC for Steel Construction (HKB).

1. Introduction

With the advancement in the metallurgical technology of the modern steel-making industry over the past few decades, various grades of structural steels have been produced successfully in many parts of the world. Owing to their high strength to self-weight ratios, high strength steels are very attractive to structural engineers to design and to build structurally efficient structures. Currently, structural steels are manufactured to various material specifications, in order to fulfil different technical requirements as stipulated in various Codes of Practice and design standards for structural design all over the world, such as EN 1993-1-1:2005 [1]. The most commonly material specifications include EN 10025-1:2005, ASTM A36, ASTM A572, AS/NZ 3679, and JIS G 3106 & JIS G 3144 [2-7], covering the technical requirements on both normal strength and high strength structural steels. In general, the mechanical requirements of normal grade structural steels are stipulated as follows:

i) the tensile to yield strength ratio, $f_u/f_y \geq 1.10$; (1a)
ii) the strain at fracture, $\varepsilon_L \geq 15\%$; and (1b)
iii) the strain corresponding to tensile strength, $\varepsilon_u \geq 15 f_y/E_s$. (1c)

For S690 steels, the strain at fracture, ε_L, is recommended to be equal to or larger than 10%

while the tensile to yield strength ratio, f_u / f_y, should be larger than 1.05 according to EN 1993-1-12: 2007 [8]. These requirements provide specific guidance to qualify high strength S690 steels for structural application.

1.1. True stress strain curves for engineering application

For structural engineering application, bi-linear stress strain characteristic is commonly adopted for structural analysis and design, in order to give safe and conservative design solutions. However, the analytical solutions often under-predict the structural capacities by 15 to 25%, adopting the nominal design values of mechanical properties and geometrical dimensions. Moreover, the load deformation characteristics of the building structures cannot be accurately predicted. Thus, non-linear stress strain characteristics, such as the Ramberg-Osgood model [9], is adopted for advanced structural analysis for structures undergoing small deformations, i.e. up to a strain at 5%. However, a full-range true stress-strain curve is required for numerical studies of structural elements with a large deformation until fracture.

Thereafter, empirical methods namely i) Linear Law; and ii) Power Law [10] were derived to provide standard non-linear true stress-strain curves after the onset of necking for investigations into ductile metal damage. However, the accuracy of these empirical methods was often found to be unsatisfactory, and hence, *Weighted Average Method* was developed [11] to correct the true stress-strain curves derived by both Linear Law and Power Law using weighted constants after direct calibration with the predicted against the measured load deflection curves.

1.2. Determination of true stress strain curves from standard tensile tests

An accurate true stress-strain curve is always essential for advanced numerical simulation of load deformation characteristics of structural members. In general, true stress-strain curves should be obtained from standard tensile tests. The true stress strain curve is commonly derived using a well-known integration method up to the onset of necking, based on a constant volume assumption.

$$\text{True strain, } \varepsilon_t = ln(1 + \varepsilon_{eng}); \tag{2a}$$

$$\text{True stress, } \sigma_t = \sigma_{eng}(1 + \varepsilon_{eng}) \tag{2b}$$

where ε_{eng} is the engineering strain = axial deflection / gauge length

σ_{eng} is the engineering stress = Applied force / Initial cross sectional area A_0

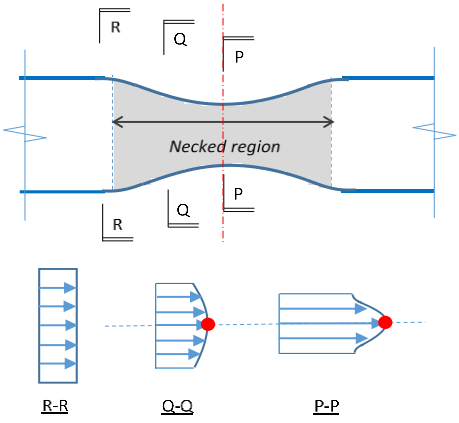

Figure 1. Typical non-uniform distribution of stresses and strains in the neck of a deformed coupon.

Figure 2. Typical set-up of a standard tensile test with precision measurements.

For deformations beyond the onset of necking, researchers commonly adopted Bridgman's correction method [10] to obtain the true stress strain curves based on test data. It should be noted that Bridgman is the first researcher to provide analytical solutions to tackle the non-uniform stress distribution across the neck of the tensile coupon under very large deformation, i.e. after the onset of

necking (Figure 1). However, high precision measurement is required to measure the instantaneous geometry and dimensions of the tensile coupon at different strain levels, resulting in the hindrance of the wide adoption of the Bridgman's correction method in the past few decades. With the advancement of the digital imaging technology and advanced image analytics, instantaneous dimensions of test coupons over the entire deformation range of tensile coupons are readily measured by authors. And hence, a new investigation method has been developed for the derivation of the true stress-strain curves of steels allowing for the effects of non-uniform stress-strain distributions within the neck of tensile coupons, namely **Instantaneous Area Method** (iAreaM) [12-14]. In this method, high-resolution digital image analytics were applied to obtain the instantaneous dimensions of the necking areas. Based on an assumption of volume conservation of the test coupons, full-range true stress-strain curves of the test steels are readily obtained through successive approximations using correction factors obtained from numerical results. Moreover, a linear continuum damage evolution model is incorporated for numerical simulation of crack propagation up to fracture.

1.3. Micrographic studies of structural steels

Metallurgists commonly conduct material characterization in different phases of steels with different volumetric fractions. These methods include dilatometry tests, 3-D micro-polycrystal structural analyses using scan electronic microscopes (SEM) and electron backscattering diffraction colour coding (EBSD) to estimate these microstructural volumetric fractions. It is widely recognized that mechanical properties of structural steels are highly dependent to their microstructures, which is controlled by the chemical compositions and the heat treatment sequence during steel-making [15-17]. It is generally recognized that normal grade as rolled steels are ferrite-Pearlitic steels possessing of normal yield strength, i.e. S275 ~ S355, with good ductility, while high strength quenched and tempered steels are martensitic steels possessing of relatively high yield strength, i.e. S690 ~ S960, with good ductility. In order to facilitate the development of our metallurgical understanding, it is essential to quantify the constitution of various phases of the structural steels, and hence, to give an accurate description of the microstructures of structural steels.

1.4. Objectives and scope of work

Other the basic mechanical properties, full true stress-strain characteristics of typical structural steels are also very important for advance numerical simulation of steel structures subjected to very large deformation up to fracture.

In order to correlate the mechanical properties of structural steels and their microstructures, a comprehensive experimental investigation was undertaken at the Chinese National Engineering Research Centre for Steel Construction (Hong Kong Branch). The following forms of experimental investigation were conducted:

- Standard tensile tests
  A total of 9 tensile tests of normal strength and high strength steels, including S275, S355 and S690 steels, were carried out to determine a generalized constitutive model for structural steels.
- Micrographic studies
  Microstructures of all tested coupons were closely examined by scanning electron microscopes to determine the volumetric fraction of various phases using Digital Image Analytics.
- Advanced numerical simulation
  Finite element models of test coupons using ABAQUS 6.13 [18] were established for detailed stress and strain analysis to determine the most critical von Mises stresses and the corresponding equivalent plastic strains within the neck of the test coupons under different levels of deformation.

2. Standard tensile tests

A total of nine standard tensile tests of S275, S355 and S690 steels to BS EN 10025-6:2005 in a standard size and shape were conducted to investigate their basic mechanical properties in accordance with standard testing procedures to BS EN ISO 6892-1:2009. Figure 2 illustrates a typical set-up of a standard

tensile test using INSTRON 8803 universal testing system. The instantaneous dimensions of the test coupons were measured using a high resolution digital imaging system as shown in Figure 3. The basic mechanical properties are summarized in Table 1, while the measured engineering stress-strain curves are plotted in the same graph for direct comparison as shown Figure 4. The average yield strengths f_y of S275, S355 and S690 coupons are found to be 352N/mm^2, 378N/mm^2, and 740N/mm^2, respectively. Their tensile strengths f_u are found to be 517N/mm^2, 550N/mm^2, and 784N/mm^2, respectively. It is shown that all tensile to yield strength ratios f_u/f_y are found to be larger than 1.1. It should also be noted that for all these coupons, the average elongation at fracture, ε_L, is found to be larger than 15%. Moreover, the strains corresponding to tensile strengths, ε_u are larger than 15 f_y / E_s. Consequently, all these coupons are demonstrated to fulfil all the ductility requirements stipulated in the Structural Eurocodes.

Table 1. Standard tensile test results.

Test	Yield strength f_y (N/mm^2)	Young's modulus E_s (kN/mm^2)	Tensile strength f_u (N/mm^2)	Strain at f_u ε_u (%)	f_u / f_y	15 ε_y (%)	Strain at fracture ε_L (%)
S275-1	354	212	514	35.0	1.45	2.60	33.9
S275-2	350	211	518	32.9	1.48	2.58	34.3
S275-3	350	210	517	34.6	1.47	2.64	34.0
Average	***352***	***211***	***517***	***34.2***	***1.47***	***2.67***	***34.1***
S355-1	382	203	556	23.8	1.49	2.75	27.6
S355-2	371	204	543	22.9	1.49	2.68	25.6
S355-3	382	205	550	22.7	1.43	2.80	28.8
Average	***378***	***204***	***550***	***23.1***	***1.47***	***2.74***	***27.3***
S690-1	739	209	776	6.69	1.05	5.30	17.4
S690-2	750	210	799	5.10	1.07	5.36	16.9
S690-3	730	209	777	4.78	1.06	5.24	16.1
Average	***740***	***209***	***784***	***5.52***	***1.06***	***5.30***	***16.8***

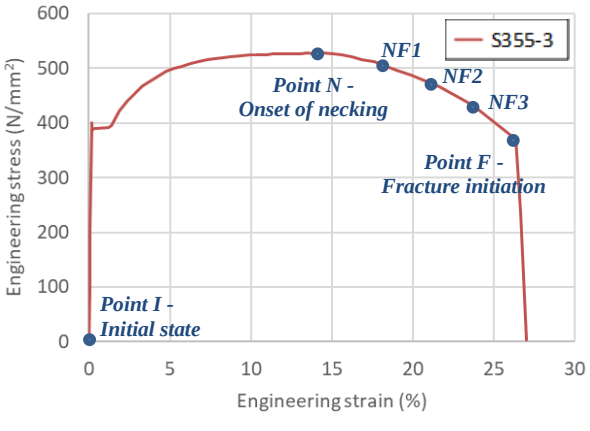

a) A typical load deflection curve of a S355 tensile coupon

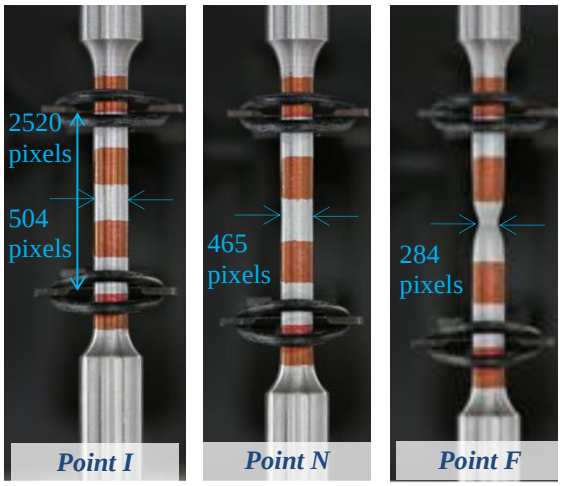

b) Measuring instantaneous dimensions and strains of a S355 tensile coupon.

Figure 3. Measurement of instantaneous dimension of a test coupon under various strains.

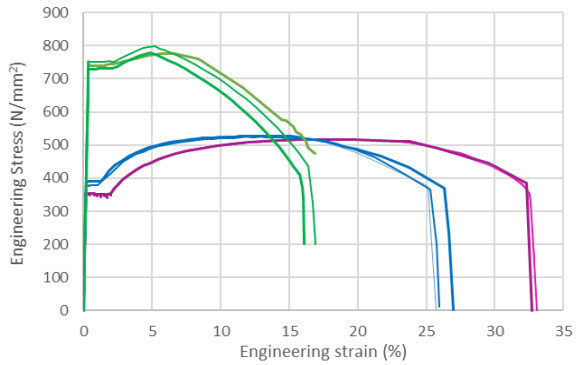

Figure 4. Engineering stress strain characteristics of typical S275, S355, and S690 steels.

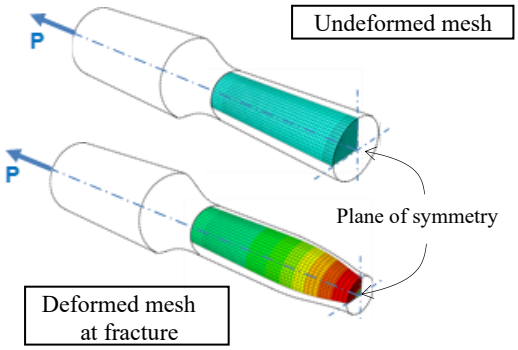

Figure 5. Advanced finite element model of test coupons with ductile damage evolution.

3. Micrographic investigation into typical structural steels

Adopting the conventional material characterization techniques, the microstructure of the S275, S355, and S690 steels were carefully examined as shown in Figure 6. Volumetric fractions of various phases within a representative area of 500µm x 500µm were evaluated using a generic Java-based image processing program software "ImageJ" for each specimen, known as Digital Image Analytics. Hence, the following key findings are obtained:

- For S275 steels, they are recognized as ferritic-pearlitic steels at the volumetric fractions of 75.5% and 24.5% respectively;
- For S355 steels, they are recognized as ferritic-pearlitic steels at the volumetric fractions of 71.0% and 29.0% respectively;
- For S690 steels, they are recognized as tempered martensite at a volumetric fraction of 99.0% together with retained austenite.

For normal grade as-rolled steels, it should be noted that their mechanical properties are sensitive to the volumetric fractions of ferrite and pearlite. The deviation of 4.5% in volumetric fractions of steel phases leads to a significant reduction in yield strength and improvement to their ductility. Further investigation is necessary to correlate the microstructural change against different mechanical properties.

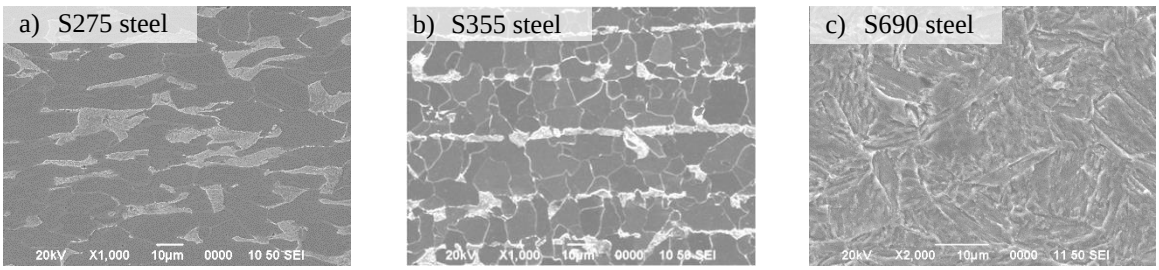

Figure 6. Micrograph of S275, S355 and S690 steels.

4. Determination of true stress-strain characteristics using Instantaneous Area Method

Instantaneous Area Method [11-13] is adopted to determinate the true stress-strain characteristics of the tested S275, S355, and S690 steels. The tri-axial stress-strain states of the core of the neck under different strain levels are evaluated using advanced numerical modelling technique (Figure 5). As such, both stress and strain correction factors are obtained using the following formulae:

$$\text{Stress correction factor} \quad \eta_\sigma = \frac{\sigma_{vm,max}}{\sigma_{av}} \tag{3a}$$

$$\text{Strain correction factor} \quad \eta_\varepsilon = \frac{\varepsilon_{p,max}}{\varepsilon_{av}} \tag{3b}$$

where $\sigma_{vm,max}$ is the maximum von Mises stress of the critical cross section;
σ_{av} is the average direct stress across the critical cross section;
$\varepsilon_{p,max}$ is the maximum principal true strain of the critical cross section;
$\varepsilon_{p,av}$ is the average direct strain across the critical cross section.

Hence, the effect of non-uniform distribution of stress and strain within the neck can be quantified by these factors, and then, both the true stress and true strain of the tested steels are readily determined. For details of the work flow using Instantaneous Area Method, please refer to Figure 7. The stress-strain non-uniformities within the neck of the S355 steels are illustrated graphically in Figure 8.

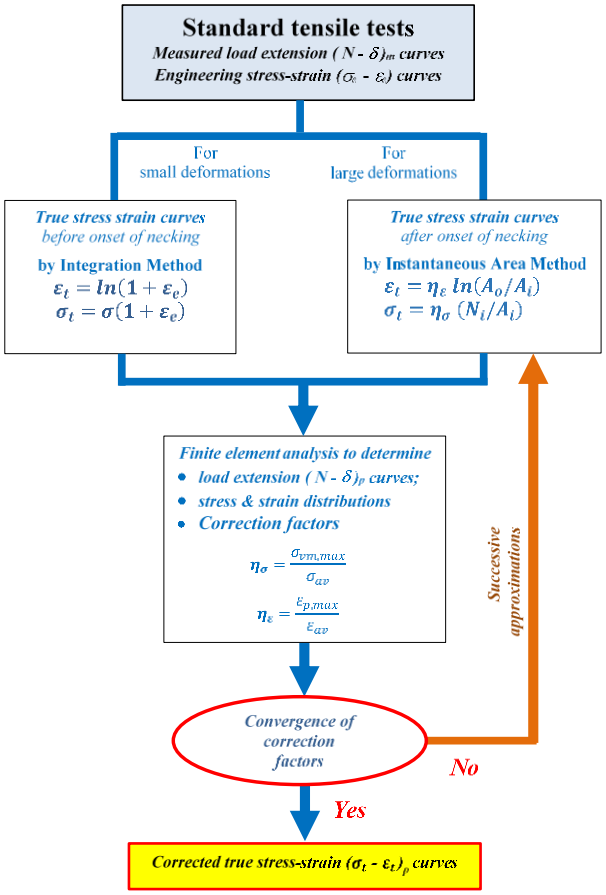

Figure 7. Flow chart of the Instantaneous Area Method with numerical correction factors through successive approximations.

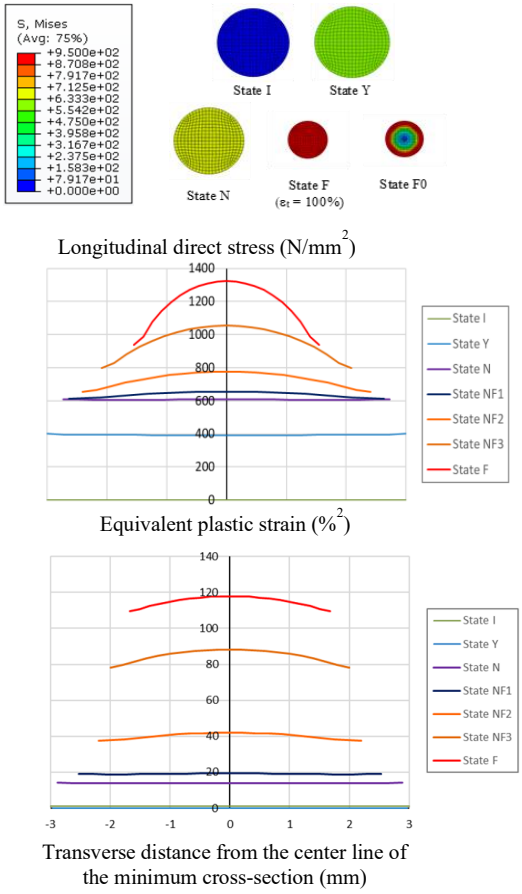

Figure 8. True stress distributions of the critical cross-section of S355-3 coupon at various deformation states.

4.1. True stress-strain characteristics of S275, S355, and S690 steels

Based on the Instantaneous Area Method, true stress-strain characteristics of S275, S355, and S690 steels are successfully determined. The true stress-strain curves of these typical structural steels are plotted in the same graph for direct comparison as shown in Figure 9a. Thus, these curves are then normalized by introducing two parameters, namely i) a normalized true stress σ_{nt}, and ii) a normalized true strain ε_{nt}, which are defined as follows:

$$\varepsilon_{nt} = \varepsilon_t E_s / f_u \quad (4a)$$

$$\sigma_{nt} = \sigma_t / f_y \quad (4b)$$

where σ_t is the true stress; ε_t is the true strain;
f_y is the yield strength; E_s is the Young's modulus; and

σ_{nt} is the normalized true stress.

All normalized true stress-strain curves are plotted onto the same graph in Figure 9b for direct comparison.

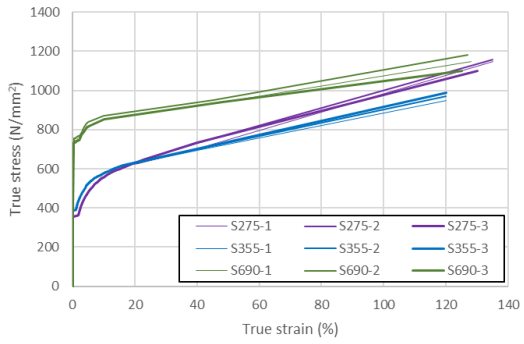

Figure 9a. Truss stress strain curves of S275, S355 and S690 steels.

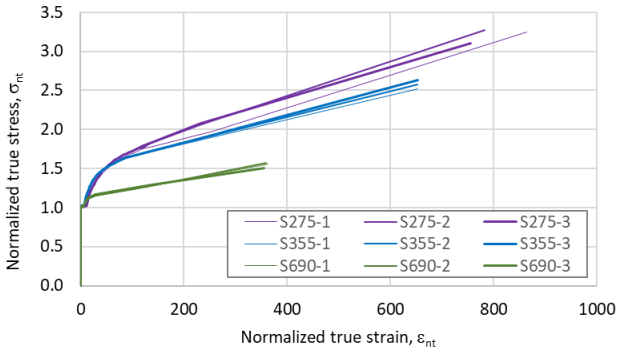

Figure 9b. Normalized truss stress strain curves of S275, S355 and S690 steels.

5. Conclusions

This paper presents both experimental and numerical investigations into mechanical properties of typical structural steels under monotonic action. Digital Image Analytics was adopted in standard tensile tests to obtain instantaneous dimensions of the test coupons over the entire deformation ranges in order to provide test data for determination of the true stress-strain curves. Based on the numerical results, non-uniform stress-strain distributions across the minimum cross-sections of the finite element models are found. Hence, the true stress-strain characteristics of these typical structural steels are successfully obtained using Instantaneous Area Method. Moreover, the microstructures of these structural steels were carefully examined, and thus, various phase constituents of the steels are successfully quantified in terms of volumetric fractions using Digital Image Analytics.

The research findings provide important experimental data for further establishment of full deformation range constitutive models for structural steels up to fracture, which enables advanced structural analysis of steel structures undergoing very large deformation. Further investigation is necessary to correlate the microstructural change against different mechanical properties.

Acknowledgement

The authors would like to express our gratitude for the financial support provided by the Research Grants Council of the Government of Hong Kong SAR (Project Nos. 152231/17E and 152157/18E). The research work on high strength steels was also partially funded by the Chinese National Engineering Research Centre for Steel Construction (Hong Kong Branch) (Project No. 1-BBY3) of the Hong Kong Polytechnic University.

References

[1] BS EN 1993-1-1:2005 *Eurocode 3: Design of Steel Structures - Part 1-1: General Rules and Rules for Buildings* (British Standard Institution)

[2] BS EN 10025-1: 2004 *Hot Rolled Products of Structural Steels – Part 1: General Technical Delivery Conditions* (British Standards Institution)

[3] ASTM A36/A36M-12 *Standard Specifications for Carbon Structural Steel* (ASTM International, 100 Barr Harbor Drive, PO Box C700, West Conshohockem, PA)

[4] ASTM A572/A572M-18. *Standard Specifications for High-Strength Low-Alloy Columbium-Vanadium Structural Steel* (ASTM International, 100 Barr Harbor Drive, PO Box C700, West Conshohockem, PA)

[5] AS/NZ 3679.1:2010. *Structural Steel Part 1: Hot-Rolled Bars and Sections* (Standards Australia,

GPO Box 476, Sydney, NSW 2001 and Standards New Zealand, Private Bag 2439, Wellington 6140)
[6] JIS G 3106: 2004 *Rolled Steels for Welded Structure* (Japanese Standards Association)
[7] JIS G 3114: 2016 *Hot-Rolled Atmospheric Corrosion Resisting Steels for Welded Structure* (Japanese Standards Association)
[8] BS EN 1993-1-12:2007 *Eurocode 3: Design of Steel Structures - Part 1-12: Additional Rules for the Extension of EN1993 up to sSteel Grades S700* (British Standard Institution)
[9] Ramberg W and Osgood W R 1943 Description of stress–strain curves by three parameters *Technical Note No. 902* (National Advisory Committee For Aeronautics Washington DC)
[10] Ling Y 1996 *AMP J. Technol.* **5** 37-48
[11] Bridgeman P W 1952 *Studies in Large Plastic Flow and Fracture* (McGraw-Hill, New York, U.S.A.)
[12] Ho H C, Chung K F, Liu X, Xiao M, and Nethercot D A 2019 *Eng. Struct.* **192** 305-22
[13] Ho H C, Liu X, and Chung K F, Xiao M, Yam M C H and Nethercot D A 2018 *Proc. Int. Conf. on Engineering Research and Practice for Steel Construction (Hong Kong)* p 160-7
[14] Ho H C, Xiao M, Hu Y F, Guo Y B, Chung K F, Yam M C H, and Nethercot D A 2020 *J. Const. Steel Research* **174** 106275
[15] Krauss G 1980 *Principles of Heat Treatment of Steel* (American Soceity for Metals)
[16] Dieter G E Jr 1961 *Mechanical Metallurgy* (New York-McGraw-Hill Book Company)
[17] Easterling K E 1992 *Introduction to the Physical Metallurgy of Welding* (Butterworth-Heinemann)
[18] ABAQUS 2013 *Analysis User's Manual Version 6.13* (Dassault Systèmes Similia Inc. U.S.A.)